Since January 2020 Elsevier has created a COVID-19 resource centre with free information in English and Mandarin on the novel coronavirus COVID-19. The COVID-19 resource centre is hosted on Elsevier Connect, the company's public news and information website.

Clinical Immunology 170 (2016) 9–19

Contents lists available at ScienceDirect

Clinical Immunology

journal homepage: www.elsevier.com/locate/yclim

Demyelinating strain of mouse hepatitis virus infection bridging innate and adaptive immune response in the induction of demyelination

Kaushiki Biswas [a], Dhriti Chatterjee [a], Sankar Addya [b], Reas S. Khan [c], Lawrence C. Kenyon [d], Alexander Choe [e], Randall J. Cohrs [e], Kenneth S. Shindler [c], Jayasri Das Sarma [a,*,1]

[a] Department of Biological Sciences, Indian Institute of Science Education and ResearchKolkata (IISER-K), India
[b] Kimmel Cancer Centre, Thomas Jefferson University, Philadelphia, PA, USA
[c] Scheie Eye Institute and FM Kirby Centre for Molecular Ophthalmology, University of Pennsylvania, Philadelphia, PA, USA
[d] Departments of Anatomy, Pathology and Cell Biology, Thomas Jefferson University, Philadelphia, PA, USA
[e] Department of Neurology and Microbiology, University of Colorado School of Medicine, Aurora, CO, USA

ARTICLE INFO

Article history:
Received 16 November 2015
Received in revised form 23 May 2016
accepted with revision 5 July 2016
Available online 6 July 2016

ABSTRACT

The presence of immunoglobulin oligoclonal bands in the cerebrospinal fluid of Multiple Sclerosis (MS) patients supports the hypothesis of an infectious etiology, although the antigenic targets remain elusive. Neurotropic mouse hepatitis virus (MHV) infection in mice provides a useful tool for studying mechanisms of demyelination in a virus-induced experimental model of MS. This study uses Affymetrix microarray analysis to compare differential spinal cord mRNA levels between mice infected with demyelinating and non-demyelinating strains of MHV to identify host immune genes expressed in this demyelinating disease model. The study reveals that during the acute stage of infection, both strains induce inflammatory innate immune response genes, whereas up-regulation of several immunoglobulin genes during chronic stage infection is unique to infection with the demyelinating strain. Results suggest that the demyelinating strain induced an innate-immune response during acute infection that may promote switching of Ig isotype genes during chronic infection, potentially playing a role in antibody-mediated progressive demyelination even after viral clearance.

1. Introduction

Multiple Sclerosis (MS) is a demyelinating disease of the central nervous system (CNS), pathologically characterized by loss of myelin, oligodendroglial cells, and axonal degeneration [1]. MS is conventionally believed to be an autoimmune disease, mediated by anti-myelin T cells and autoantibodies. Although the etiology is unknown, indirect evidence such as the presence of oligoclonal bands (OCBs) and abnormally increased levels of immunoglobulins (Ig's) in CNS tissue and cerebrospinal (CSF) fluid of MS patients suggest that viral infections play a role in triggering the disease process. Various experimental animal models of virus induced demyelination exist, including the demyelinating strain MHV-A59, and its recombinant demyelinating strain, RSA59 induced demyelination in C57Bl/6 mice [2–5]. Upon intracranial inoculation, RSA59 causes a biphasic disease that mimics some MS pathology. In the acute phase, RSA59 causes neuroinflammation including meningitis, encephalitis, myelitis and sparse demyelination. Myelin loss starts as early as day 5 post-innoculation (p.i.) but reaches its peak by days 25–30 (chronic disease phase), when infectious viral particles are below the limit of detection and viral antigen has resolved, but viral RNA persists [2,6,7]. Demyelination and axonal loss depend on the viral host-attachment spike protein, as RSMHV2, a closely related isogenic strain that differs from RSA59 only in the spike gene, can cause meningitis, encephalitis, myelitis and occasional optic neuritis [8] but is unable to cause demyelination or axonal loss. Thus, spike plays a major role in MHV-induced myelin loss and axonal loss, but it is unknown how differences in spike affect gene expression in order to mediate different host tissue responses. Our recent studies using Affymetrix microarray analysis revealed that RSA59 induces IFN-gamma inducible genes and innate immune-activating pathway genes during the acute stage of infection [9]. Recent studies using a high-throughput RNA–Seq approach also revealed expression of several genes involved in macrophage function, immune infiltration, and changes in cytokine expression levels in response to persistent MHV infection in mice [10].

However, no high-throughput expression studies are available to identify host immune response genes in the chronic stage of infection,

* Corresponding author at: Indian Institute of Science Education and ResearchKolkata (IISER-K), Mohanpur-741246, West Bengal, India.
E-mail address: dassarmaj@iiserkol.ac.in (J. Das Sarma).
[1] Adjunct: Department of Ophthalmology, University of Pennsylvania; Department of Anatomy, Pathology and Cell Biology, Thomas Jefferson University, Philadelphia, Pennsylvania, USA.

http://dx.doi.org/10.1016/j.clim.2016.07.004
1521-6616/

when demyelination and axonal loss are major pathological hallmarks. In the current studies, we examined changes in gene expression in the spinal cord during acute and chronic stage of DM (demyelinating; RSA59) and NDM (non-demyelinating; RSMHV2) MHV infection.

2. Results

2.1. Acute and chronic pathology of mice infected with DM and NDM strains

Four week old C57BL/6 mice were inoculated intracranially with DM (RSA59) or NDM (RSMHV2) strains using the LD_{50} as described in prior studies [10–12]. To confirm infection, histopathology and immunohistochemistry were performed on liver, brain and spinal cord sections from mice whose spinal cords were processed for Microarray analysis. Both strains induced hepatitis (score 2–3 on a relative scale [11]) (Fig. 1B and C), and mock-infection induced none (score 0) (Fig. 1A). No encephalitis was observed by H&E staining of control mouse brains (Fig. 1D), but there was encephalitis, characterized by activated microglia/macrophages (stained for Iba-1) [12,13] in olfactory bulb, basal forebrain (Fig. 1E and F), hippocampus, basal pons and deep cerebellar white matter at day 6 p.i. with DM and NDM strains. At day 25 p.i., DM strain induced myelin loss, evident by LFB staining (Fig. 1H), but NDM strain did not (Fig. 1I). Parallel sections stained with Iba1 showed accumulation of microglia/macrophages in demyelinating plaques (Fig. 1K) of DM strain infected, but not in NDM infected, mouse spinal cords (Fig. 1L).

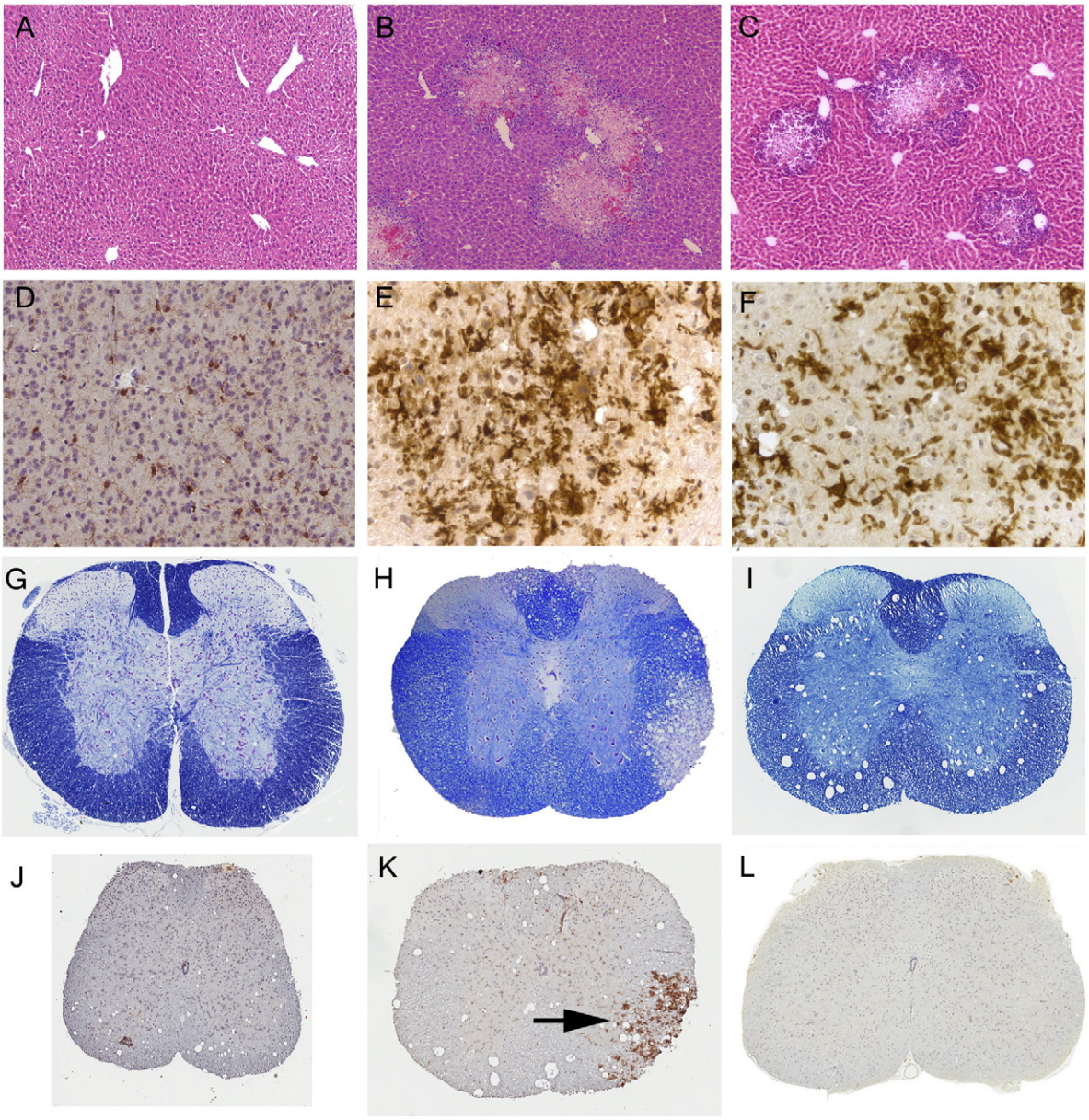

Fig. 1. Histopathology and immunohistochemical analysis of DM and NDM-infected mouse liver, spinal cord and brain respectively. A, D, G and J sections are from Mock-infected mouse; B, E, H, K are from DM infected mouse and C,F,I and L are from NDM infected mouse. A: liver tissues stained with Hematoxylin & Eosin show no hepatitis but B and C: liver tissues stained with Hematoxylin & Eosin show moderate to severe hepatitis in both DM (B) and NDM (C) infected mice at 6 days p.i. E and F: Sagittal brain sections during acute infection (day 6 p.i.) from both DM (E) and NDM (F) infected mice immunostained with anti-Iba-1 show vast accumulation of Iba-1 + (microglia/macrophage) cells in the basal forebrain. D: Sagittal brain sections during acute infection from mock infected mouse and only resident microglial staining was observed. H and I: Luxol Fast Blue stained spinal cord sections demonstrate demyelinating plaque in DM strain infected mice (H) but no demyelination in NDM strain infected mice (I) in the chronic phase of infection (day 25 p.i.). No demyeliantion was also observed in the spinal cord section of mock infected mouse (G). Parallel sections in DM strain infected mice (K) demonstrate Iba1 + cells present in the demyelinating plaque (arrow). In the mock (J) and NDM strain very few Iba-1 + cells were present at day 25 p.i. (L).

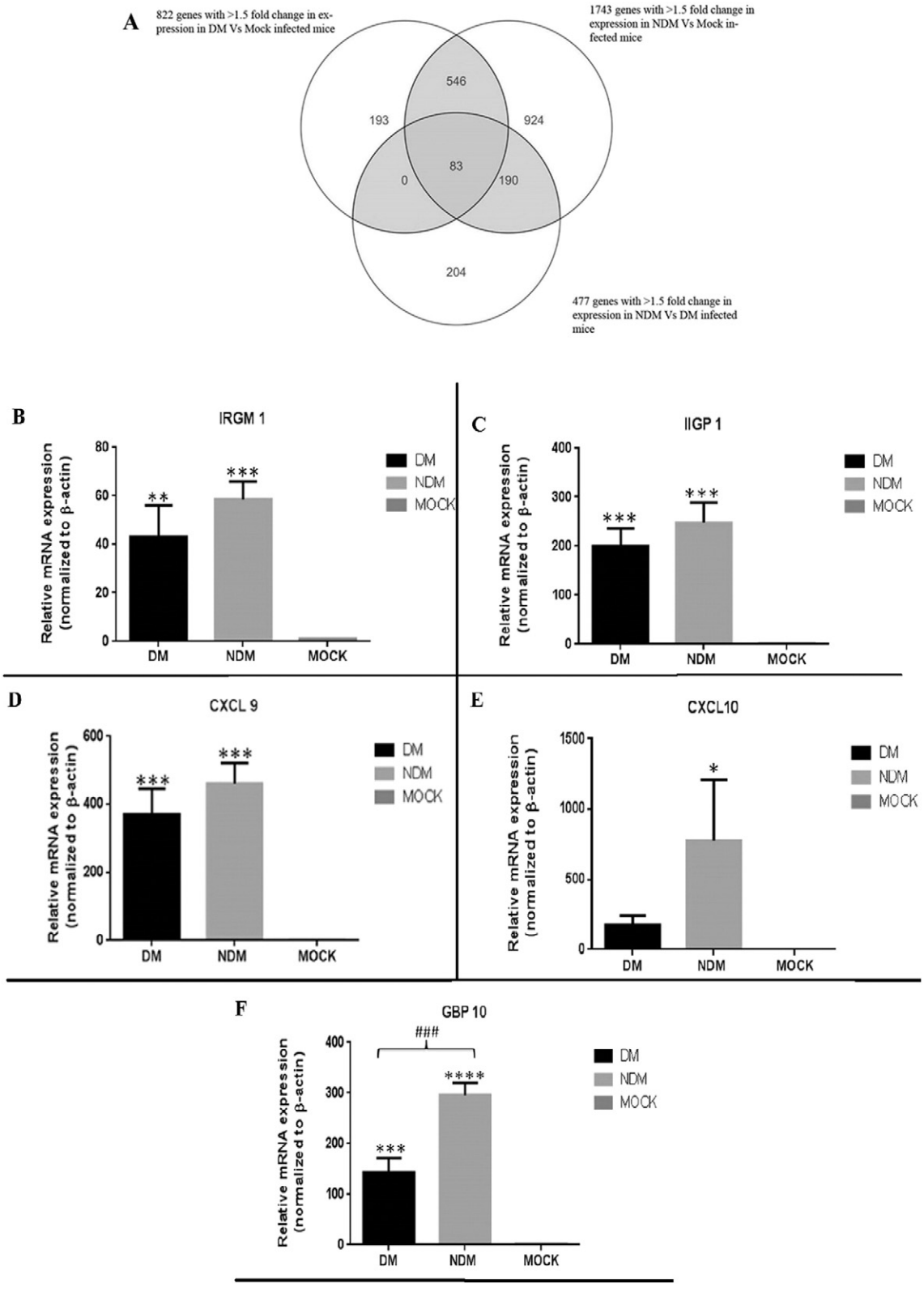

Fig. 2. Differentially expressed genes at day 6 p.i. in spinal cords from DM, NDM and mock infected mice. A. Venn diagram depicts number of genes whose expression changed by at least 1.5 fold during DM strain infection (left circle) compared to mock infected controls, during NDM infection (right circle) compared to mock infected controls, and during DM strain infection compared to NDM infection (bottom circle). Overlapping changes between more than one comparison group is shaded. B. Increased expression of specific genes found to be upregulated by microarray analysis, including IRGM 1 (B), IIGP 1 (C), CXCL 9 (D), CXCL 10 (E), and GBP 10 (F) were validated by quantitative real time PCR. The fold change in gene expression with respect to mock infected mice ($2^{-\Delta\Delta Ct}$) was calculated for each of the genes in DM and NDM strain infected mice and plotted. Results show significant upregulation of all genes examined ($^{*}p < 0.05$; $^{**}p < 0.01$, $^{***}p < 0.001$, $^{****}p < 0.0001$) as compared to mock infected mice. Only GBP10 showed significant differences between the DM and NDM strain ($^{\#\#\#}p < 0.001$). Stars (*) imply the gene expression was statistically significantly upregulated as compared to mock infected mice, whereas $^{\#}$ imply that there is a significant difference in the upregulation of certain genes between DM and NDM strain infection.

2.2. Upregulation of innate immune response genes at acute phase of DM and NDM strain infection

Affymetrix microarray analysis was performed on extracts from spinal cords isolated on day 6 p.i. Genes that demonstrated significant differences in expression level were identified in comparisons between DM vs. Mock, NDM vs. Mock and DM vs. NDM infected spinal cords. Using a threshold of 1.5 fold change in expression level ($p < 0.05$), 822 genes were found to be differentially expressed in DM infected spinal cord compared to mock infected controls; whereas, in NDM strain infected spinal cord 1743 genes were differentially expressed compared to mock infection (Fig. 2A). 477 genes were differentially expressed between mice infected with DM and NDM strains. Most differentially expressed genes were upregulated both in DM and NDM strain, with few genes downregulated.

Analysis revealed that both strains induced innate immune response genes. The majority of upregulated genes are known to be involved in pathways which activate microglia/macrophages and induce interferon-gamma, and thus may be involved in antiviral activities. Detailed differential expression data is listed in Supplementary Table 1. Briefly, genes involved in microglial activation like Allograft inflammatory factor 1 (AIF 1) that encodes Iba1, Macrophage expressed gene 1, interferon-gamma inducible and activated genes including Guanylate binding proteins (GBPs), Interferon-inducible GTPase, Immunity-related GTPase M proteins (IRGMs), Interferon regulatory factors (IRFs), various Interleukins, chemokines and chemokine receptors and MHCs were upregulated. CD antigens like CD74, CD3, CD52 and CD274 were also upregulated in both DM and NDM strain infection. Toll-like receptor (TLR) family members TLR 1, 2, 4, 7 and 9 and some NLR family genes were upregulated, most prominently NLR family member CARD domain containing 5 that is implicated in anti-viral immunity and MHC class I expression regulation. Overall, most innate immune response genes were upregulated by both NDM and DM, with a trend toward greater upregulation in NDM strain infection, but differences were not significant, except for one gene, *GBP10*.

2.3. Quantitative real time PCR (qRT-PCR) confirms gene upregulation

qRT-PCR was performed on the same spinal cord RNA used for microarray analysis in order to confirm whether observed changes in expression were significant. Expression of selected genes upregulated during acute infection, along with β-actin as endogenous control, was measured. The relative fold change of mRNAs in spinal cords of DM and NDM infected mice with respect to mock controls was calculated by the $2^{-\Delta\Delta Ct}$ method. Similar to microarray data, qRT-PCR results showed upregulation of IRGM 1 (44.7 fold in DM/58.56 fold in NDM) and IIGP 1 (200 fold in DM/247 fold in NDM) when compared to mock-infection (Fig. 2B and C). CXCL9 was also upregulated by both DM strain (369.5 fold) and NDM strain (461.8 fold) (Fig. 2D). CXCL10 was more highly upregulated by NDM strain (775.7 fold) than DM strain (175.9 fold) (Fig. 2E). GBP10 was also significantly upregulated in both DM and NDM infected mouse spinal cord during the acute stage of infection (Fig. 2F). Among those genes only GBP10 showed significant differences between the DM and NDM strain ($^{###}p < 0.001$).

2.4. Differential gene expression at chronic phase of infection identifies upregulated genes involved in adaptive immunity

Affymetrix microarray analysis was performed on extracts from spinal cords isolated on day 25 p.i. Genes that demonstrated significant differences in expression level were identified in comparisons between DM vs. Mock, NDM vs. Mock and DM vs. NDM infected spinal cords. Using a threshold of 2 fold change in expression level ($p < 0.05$), 134 genes were found to be differentially expressed in DM strain infected spinal cord compared to mock infected controls; 135 genes were differentially expressed in NDM strain infected mice compared to controls; and 40 genes were differentially expressed in DM strain infected mice compared to both mock and NDM infection (Fig. 3A). 72 differentially expressed genes were common to both DM and NDM strain infection. 22 genes were unique in DM strain infection while 63 unique genes were differentially expressed only in NDM strain infection. A complete list of differentially expressed genes during the chronic phase of infection is shown in Supplementary Table 2.

Interestingly, the 40 genes differentially expressed in DM strain infected mice relative to both mock and NDM strain infection (Fig. 3B) did not show any differential expression during acute phase infection. Ingenuity Pathway Analysis (IPA) demonstrates that these genes belong to pathways involved in switching of innate to adaptive immunity, including B cell development pathways and communication pathways between innate and adaptive immune systems (Fig. 4A). Evaluation of these 40 genes demonstrates that only 10 genes have functional coding regions, mostly involved in B cell development: IGHA1, Ighg3, IGHM, IGJ, Igk-V28, Igkv4-68, Igkv6-14 and SLPI (Fig. 4B). Further investigation showed that there is also upregulation of CXCL13, an important cytokine for recruitment of B cells in the CNS, in DM strain infected mice. Expression of the IGJ gene in mock, DM and NDM infected spinal cord was measured by qRT-PCR as a representative gene to validate expression levels, and results confirmed similar expression as identified by microarray (data not shown).

2.5. Unique genes expressed in chronic stage DM strain infection

The 22 genes that uniquely changed expression in chronic DM strain infection at day 25 p.i. are listed in Supplementary Table 3. The canonical pathway analysis program in the IPA software demonstrates these 22 genes are involved in B cell development pathways, T helper cell differentiation, CD40 signaling, T cell receptor signaling, and CTLA4 signaling, among others (Fig. 5), with the majority implicated in B cell development pathways. IPA Network analysis of these 22 genes identifies two important pathways: B lymphocyte activation and Ig Class switching. The most striking interactions were observed between CD3, CD45, and MHC-II, which in turn is able to promote B lymphocyte activation and Ig Class switching via CD40 signaling. Similarly, IPA Path designer network analysis demonstrates Ig isotypic molecules overexpressed in DM infection are interconnected in a B cell development network (Fig. 6). Because results show significant upregulation of genes involved in B cell development and Ig class switching, antibodies were used to detect proteins produced by specific genes (IgJ, IgA K-chain, IgHA1, Ighg3, IGHM, IgM and IgG) found to be upregulated only in DM strain infection during the chronic phase of infection (day 25 p.i.). Protein levels in CSF, where oligoclonal banding is seen in MS patients, was measured by immunoblotting, but only 10–15 μL of CSF could be collected from the infected mice which was insufficient to detect any binding (data not shown). Proteins levels were also not high enough in whole tissue lysates to detect meaningful expression above background (data not shown). Immunohistochemistry of brain sections demonstrated small areas of increased IgG (data not shown) and IgM staining in the brain of DM strain infected mice as compared to NDM strain infected and mock infected mice (Supplemental Fig. 1). In spinal cord (Supplemental Fig. 2), and other parts of the brain, more diffuse increased staining was also observed in DM strain infected mice, but high background staining levels require that these findings be interpreted cautiously.

2.6. Protein markers of innate immune response increase in both DM and NDM infection

Mouse cytokine assay analysis was performed on spinal cord tissue lysates to examine whether changes in protein expression correlate with observed gene expression changes following MHV infection. Data show that at day 6–7 p.i.(acute phase) markers for innate immune responses, including mKC (KC/GRO) and IFN-γ, are upregulated in both

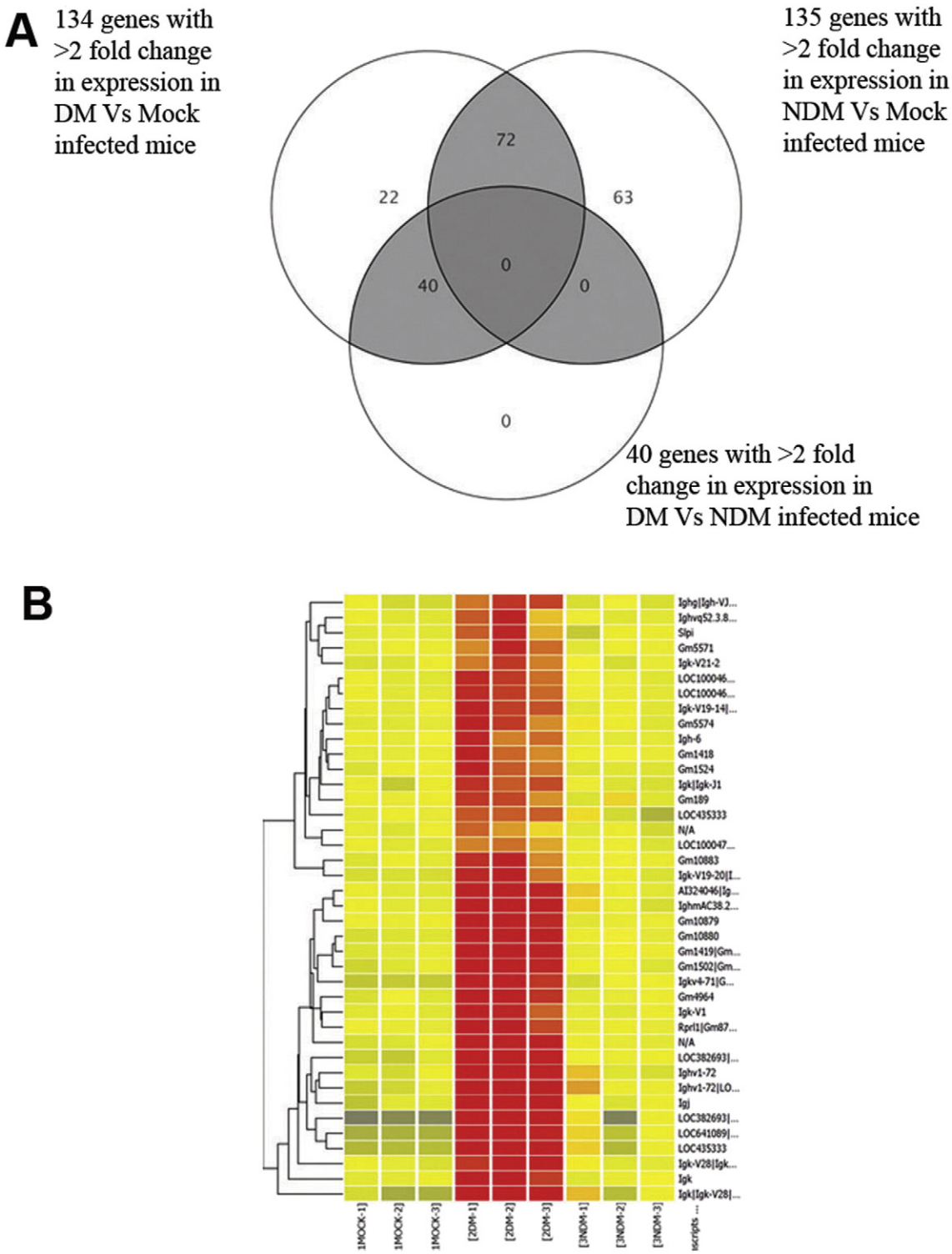

Fig. 3. Differentially expressed genes in DM, NDM and mock infected mice during the chronic phase of infection (day 25 p.i.). A. Venn diagram depicts number of genes whose expression changed by at least 2 fold during DM strain infection (left circle) compared to mock infected controls, during NDM infection (right circle) compared to mock infected controls, and during DM strain infection compared to NDM infection (bottom circle). Out of 134 genes expressed differentially in DM and 135 genes in NDM compared to mock, 72 genes are common to both DM and NDM strain infection. 22 genes are uniquely expressed in the DM strain infection. 63 genes are uniquely expressed in the NDM strain infection. 40 genes are differentially expressed in the DM strain infection uniquely when compared to NDM and mock infection. B. Heat map representing the level of expression of the 40 genes differentially expressed in DM strain as compared to both mock and NDM infected spinal cords. A spectrum of colors depict the relative gene expression levels ranging from blue color signifying low expression and moving toward red colors indicating more significant upregulation.

DM and NDM infected mice compared to controls (Fig. 7A and B), with protein levels modestly but significantly higher in NDM strain than DM strain infected mice, similar to microarray results. Levels of both proteins significantly diminish by day 26 p.i. Cytokine assay for Th1 and Th2 cytokines IL-12 and IL-10, respectively, also reveal significant upregulation following both DM and NDM strain infection (Fig. 7C and

A

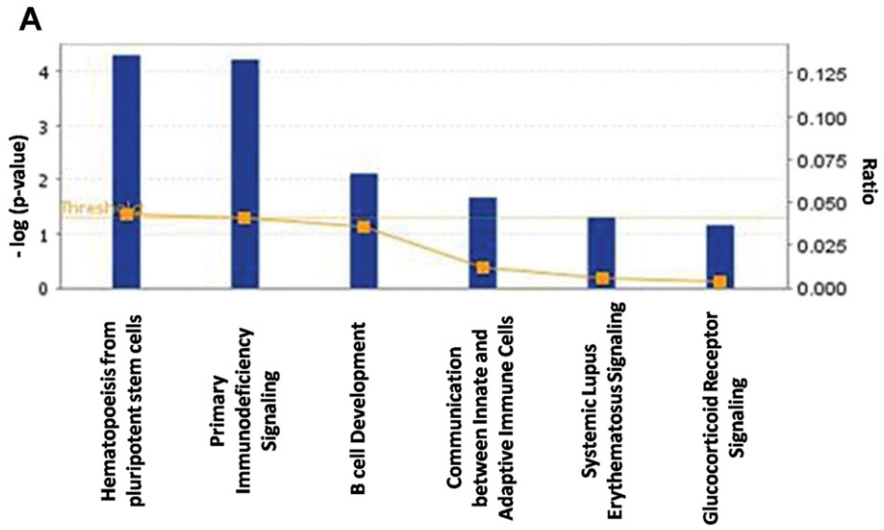

B

Gene name	Gene symbol	Fold change
Immunoglobulin heavy constant alpha 1	IGHA1	4.375 up
Immunoglobulin heavy constant gamma 3	Ighg3	10.148 up
Immunoglobulin heavy constant gamma 3	Ighg3	11.059 up
Immunoglobulin heavy constant mu	IGHM	3.441 up
Immunoglobulin J polypeptide	IGJ	21.218 up
Immunoglobulin kappa chain variable 28 (V28)	Igk-V28	39.528 up
Immunoglobulin kappa chain variable 28 (V28)	Igk-V28	8.991 up
Immunoglobulin kappa chain variable 4-68	Igkv 4-68	13.134 up
Immunoglobulin kappa chain variable 6-14	Igkv 6-14	4.727 up
Secretory leukocyte peptidase inhibitor	SLPI	3.458 up

Fig. 4. Analysis of genes differentially expressed in chronic DM strain infection as compared to both NDM and mock infected mice. A. The 40 genes that were differentially expressed in DM strain infection with respect to both NDM strain and mock infection (shown in Fig. 3B) were analyzed by Ingenuity Pathway Analysis Software, and were found to be involved in six canonical pathways, including the B cell development pathway. The *p*-value associated with a Canonical Pathway is a measure of the likelihood that there is significant association between the 40 genes differentially expressed in DM strain infection with the known set of genes involved in that given pathway. The *p*-value is calculated using the right-tailed Fisher Exact Test. The *p*-value for a given process annotation is calculated by considering (1) the number of focus genes that participate in that process and (2) the total number of genes that are known to be associated with that process in the selected reference set. The more focus genes involved, the more likely the association is not due to random chance and thus the more significant the *p*-value. Similarly, the larger the ***total*** number of genes known to be associated with the process, the greater the likelihood that an association is due to random chance, and the *p*-value accordingly becomes less significant. The smaller the *p*-values are, the less likely that the association is random and the association is more significant. *P*-values <0.05 indicate a statistically significant, non-random association and the threshold line representing the *p* value is 0.05. Canonical pathways are ranked according to their *P* value and represented as the blue bars. Ratio indicates the number of genes differentially upregulated in our data set that overlap with the particular pathway listed. B. Ten specific genes that are involved in the B cell development pathway and include various immunoglobulin isotypic genes were found to be upregulated in DM strain infection only. Each gene, along with its significant fold-upregulation in DM strain infection is shown.

D). NDM strain infected mice show dramatically statistically significant greater upregulation of mKC (KC/GRO), IFN-γ, and IL-12 at acute phase when compared to DM strain infected mice, whereas at day 26 p.i., mKC, IFN-γ and IL-12 expression in NDM strain infected mice decreases to a level equivalent to that found in DM strain infected mice. Similarly, IL-10 expression decreases sharply in NDM strain infected spinal cords during chronic infection.

3. Discussion

Infection with both DM and NDM strains of MHV-A59 induce numerous innate immune response genes at the acute stage of infection. Results in DM strain infected spinal cord are consistent with prior studies of acute infection [9], with current data showing that most of these genes are upregulated to a similar level, and one to an even greater degree, by NDM strain infection. One possible explanation for the observed induction of innate immune system genes by both viral strains may be an anti-viral immune response, as opposed to being involved in mechanisms of demyelination; that is, observed responses in both strains may reflect host attempts to clear the virus from the CNS after acute infection. Higher levels of innate immune system genes in NDM strain infection, if detected, may provide an explanation for viral persistence of the DM strain, but not the NDM strain, as observed in previous studies [4,14,15] and reconfirmed in the current study with viral nucleocapsid specific primer probe set (data not shown). This supposition remains unclear, however, as only one gene (GBP10) was confirmed to be different by RT-PCR between strains, while several proteins (mKC, IFN-γ, and IL-12) did show significantly higher upregulation between strains. Cytokine analysis revealed upregulation of IL-12 that also promotes secretion of IFN-γ, itself known for its anti-viral activity and role in viral clearance, supporting the possibility that these genes are induced specifically to control viral replication and infection. In contrast, the absence of significant differences in many other genes that are upregulated by both strains suggests that other mechanisms are likely

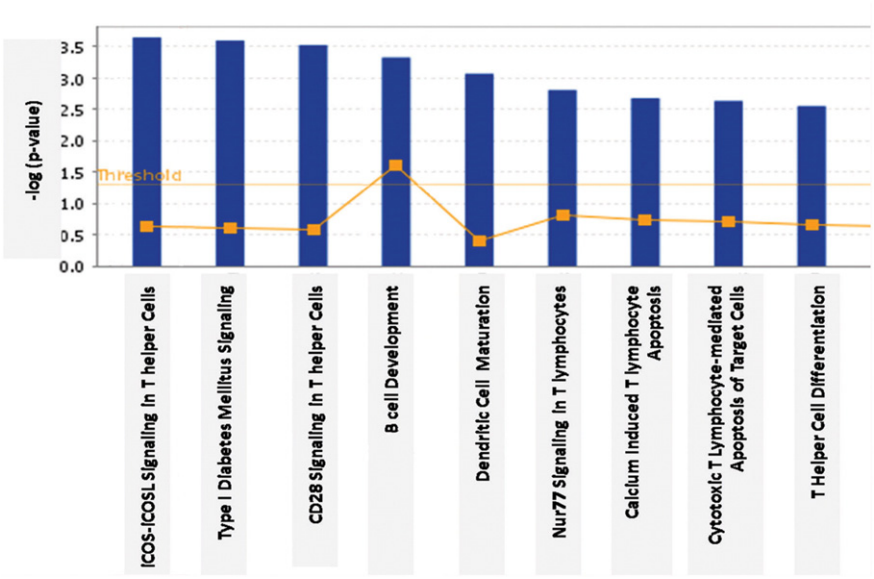

Fig. 5. Analysis of genes differentially expressed in chronic DM strain infection as compared to mock infected mice alone. A. The 22 genes that were differentially expressed in DM strain infection with respect to mock infection (Fig. 3A) were analyzed by Ingenuity Pathway Analysis Software, and are found to be involved in various canonical pathways, including T helper cell signaling and B cell development pathways. The *p*-value associated with a Canonical Pathway is a measure of the likelihood that there is a significant association between the 22 genes differentially expressed in DM strain infection with the known set of genes involved in that given pathway. *P*-values <0.05 indicate a statistically significant, non-random association and the threshold line represents the *p* value is 0.05. Canonical pathways are ranked according to their *P* value and represented as the blue bars.

involved in differential clearance; thus, our current mixed results imply that the degree of innate immune responses may only play a minor role in observed differences in viral clearance.

During the chronic phase of MHV infection, the level of expression of innate immune response genes is reduced in both strains, more drastically in NDM strain infected mice. Unlike acute innate immune response genes, genes involved in adaptive immune responses are upregulated only during the chronic stage of spinal cord infection, and only in mice infected with the DM strain. Specifically, significant upregulation of Ig genes occurs in the DM strain, and the top canonical pathways whose genes are implicated include the T helper cell signaling pathway, B cell development pathway, and communication between innate and adaptive immune cells. The upregulation of various Ig isotypic genes in DM strain infection only in the chronic phase suggests they may play a role in the chronic stage pathology, including a possible role in demyelination or axonal loss, although future studies will be necessary to determine if these genes are indeed involved in mechanisms of demyelination, or whether their expression merely changes as a consequence of the disease.

A potential relationship between demyelination and Ig's and oligoclonal bands (OCBs), as found in CSF and CNS tissues of MS patients, has long been suspected [16]. Their presence has been cited as evidence of an infectious etiology [17,18]. Though the antigenic targets of the IgG's have been difficult to confirm, various studies reported reactivity of intrathecal IgG's from MS patients to several myelin epitopes [19,20] as well as to oligodendrocytes themselves [21,22]. The current data is consistent with the possibility that viral infection may trigger CNS demyelination and induce Ig OCBs without leaving any markers to identify the specific underlying infectious agent. B cells can either be primed in the peripheral immune system with subsequent infiltration in the CNS by cytokines like CXCL13 or alternatively, they can be activated and maintained locally in CNS [23–25]. Histopathological analysis of DM and NDM strain infected mouse spinal cords, as seen in prior studies and again here, is consistent with observed patterns of viral RNA persistence and changes from innate to adaptive immune responses. In NDM strain infection, when infectious viral particles resolve in the chronic stage, activated microglia return to a quiescent stage, but in DM strain infection, viral RNA persists and inflammatory cells also remain in demyelinating plaques [26,27]. Differences observed here in expression of adaptive immune response genes lead us to hypothesize that persistence of activated microglia/macrophages identified in prior studies may help initiate the adaptive immune response during chronic DM strain infection.

Interestingly, current changes in immune responses observed in RSA59 spinal cord infection are similar to important results reported following infection with the more virulent, yet related, strain MHV-JHM [28–33] . Several groups have shown that the extent of MHV infection plays a critical role in inducing changes in cytokine expression, and rapid viral growth may suppress lymphocytic responses. While A59 and JHM strains have many similarities, JHM is highly neurovirulent and follows different kinetics of accumulation of virus-specific CD4+ and CD8+ T cells. Although activated microglia and macrophages make up the vast majority of early infiltrates, up to day 5 following infection in both strains, T cells are most abundant during peak of the inflammation and thereafter in MHV-JHM, whereas in RSA59 few T cells are present at the peak of inflammation [7–9,26]. Thus, it was not clear whether MHV-A59 induced changes in immune response genes would be similar to those found in MHV-JHM infection, yet our current results suggests that there indeed may be similar time courses of innate and adaptive immune responses. Future direct comparisons may be useful to further examine their similarities and differences.

One potential limitation with the current study, as with all animal studies, is how well the findings translate to human disease [34–36]. The potential translation here is enhanced by the fact that the model used mimics many of the histopathological features of MS, and by some published evidence suggesting MS may be triggered by a viral infection [18,37,38]. Thus, it might be expected that similar changes in immune regulation as found in our studies could occur in the serum and CSF of MS patients in the early phase of the first attack of demyelination versus subsequent attacks in chronic MS. Thus, understanding the timing and progressive phases of immune responses may indeed lead to identification of potential points to target with both current and novel immunomodulatory therapies.

in addition, the MHV-induced model of CNS demyelinating disease used in the current studies shares many histopathologic features with the human disease MS, as well other viral-induced and autoimmune MS animal models [3,39–42]. Features include inflammatory cell

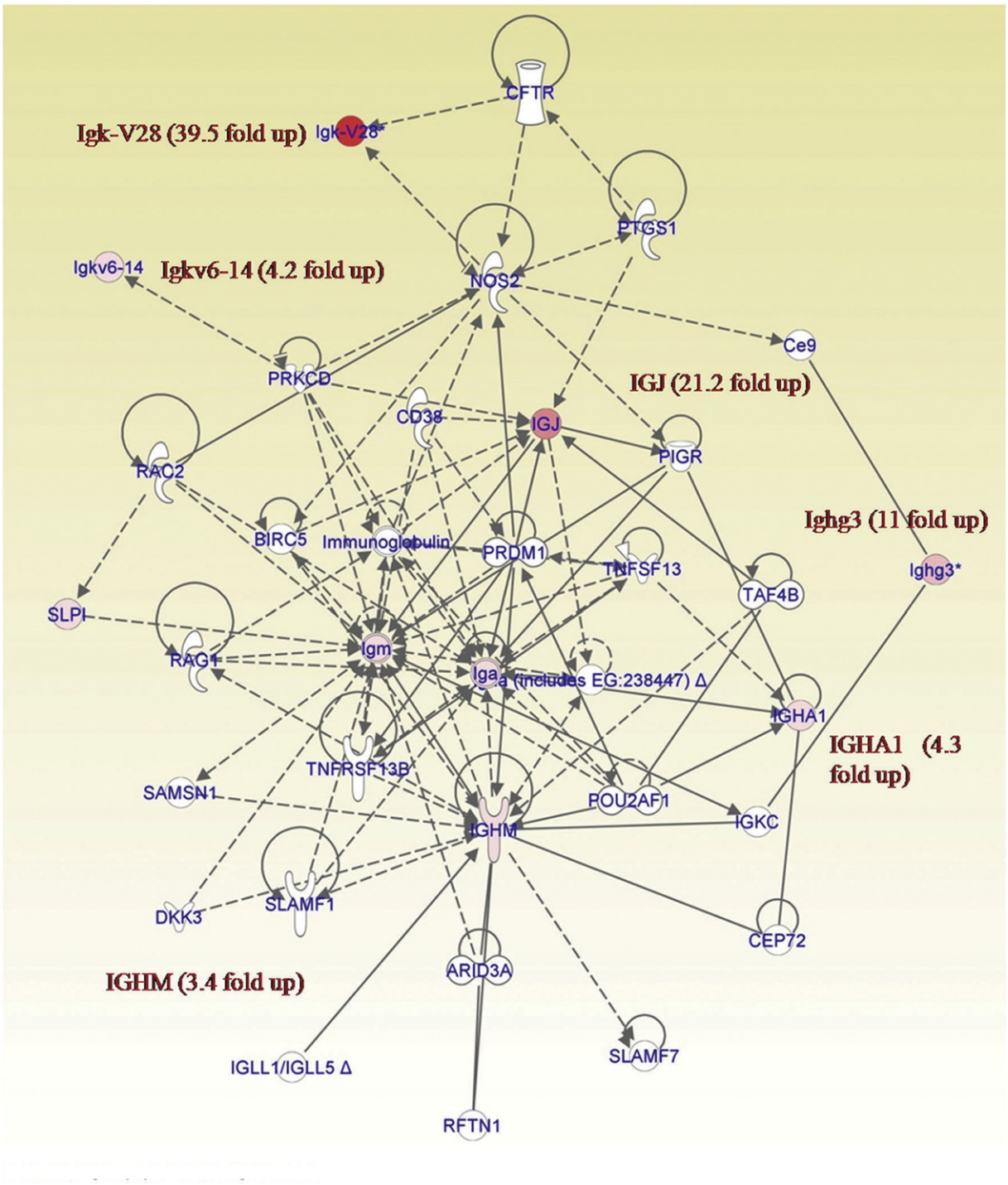

Fig. 6. Network analysis of genes differentially expressed in chronic DM strain infection. Genes that were significantly upregulated in spinal cords of DM strain infected mice were further analyzed using the Path designer network analysis function of the IPA software to identify the most significant gene network implicated by the upregulated group of genes. Results demonstrating upregulated Ig isotypic molecules are interconnected in a B cell development network. Nodes in the network represent the genes and the lines connecting the nodes represent the kind (direct is solid line; indirect is dotted line) of relationship/interaction existing between the genes. The intensity of the node color represents the degree of upregulation. Genes in uncolored nodes were not identified as differentially expressed in our experiments and are integrated into the network by the IPA software indicating their relevance to the network.

infiltration of CNS predominantly in white matter, demyelination, and truncation and swelling of axons [26,43]. The best studied virus-induced models of CNS demyelination in mice are the picornavirus TMEV and certain strains of the coronavirus MHV [2,44–47]. While these models demonstrate similar histopathology, the pathogenesis of TMEV-induced demyelination probably differs from that in MS, where persistent viral infection of the CNS has not been demonstrated, as is seen with TMEV [44]. In contrast, some neurotropic MHV strains provide models in which viral infection of the CNS is cleared and controlled by remarkably well-defined mechanisms [3,4,26]. Notably, MHV encephalitis carries a sequela of inflammatory demyelination in the absence of detectable pathogen gene expression. The elucidation of this apparent 'hit and run' demyelinating event may hold lessons for understanding MS.

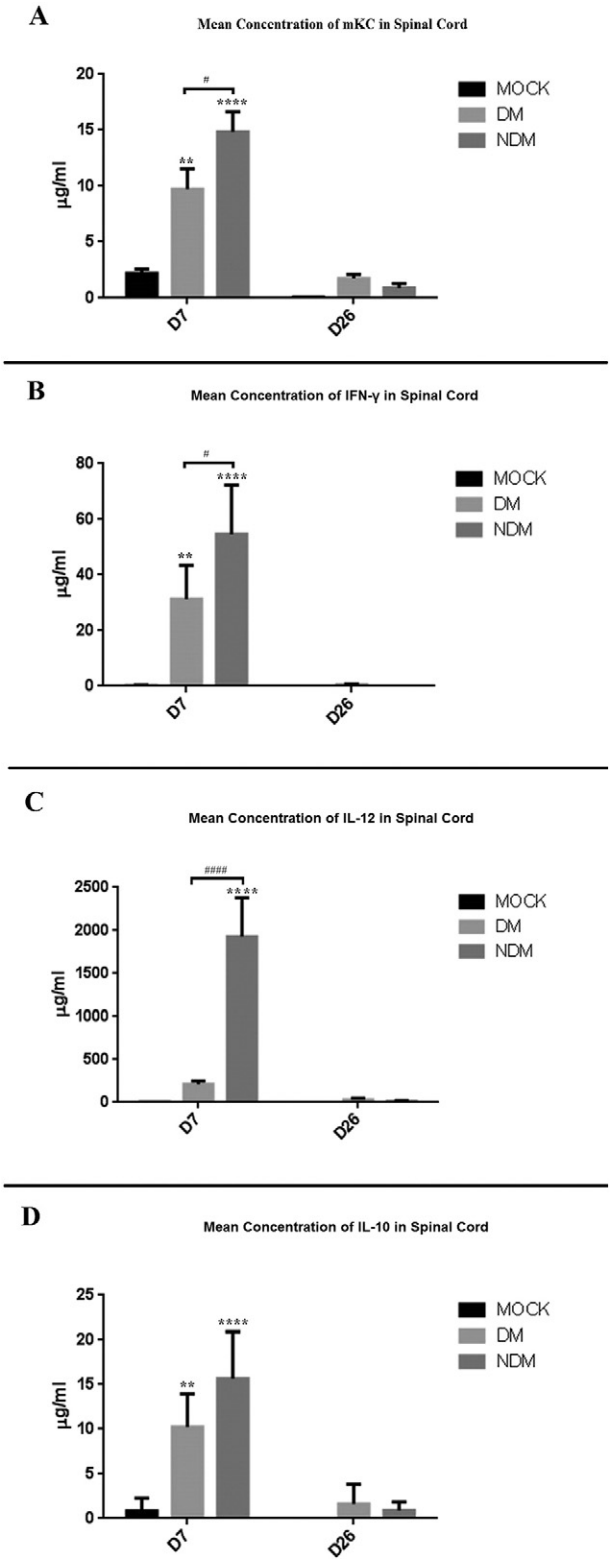

Fig. 7. Differential expression of IFN-γ, IL-10, IL-12 and mKC protein in spinal cords of DM and NDM strain infected mice during acute and chronic infection. Meso Scale Discovery (MSD) Multiarray system for mouse cytokine assay was performed using spinal cord tissue lysate from DM, NDM and mock infected mice isolated at day 7(acute stage) or day 26 p.i. (chronic stage). mKC (KC/GRO) (A), IFN-γ (B), IL-12 (C), and IL-10 (D) are all significantly upregulated during the acute phase of NDM infection and mKC (KC/GRO) (A), IFN-γ (B),) and IL-10 (D) are significantly upregulated during the acute phase of DM strain infection ($^{*}p < 0.05$; $^{**}p < 0.01$, $^{***}p < 0.001$, $^{****}p < 0.0001$) as compared to mock infection; whereas in the chronic phase, levels are much lower than in the acute phase. There are significant differences between DM and NDM strain infection for the expression of mKC ($^{\#}p < 0.05$), IFN-γ($^{\#}p < 0.05$) and IL-12 ($^{\#\#\#\#}p < 0.0001$), as determined by two way ANOVA.

In conclusion, the current studies show that innate immune responses induced in the acute phase surrender to development of adaptive immune responses in the chronic phase of RSA59 DM strain infection, and suggest potential pathways that should be explored as possible precipitating events leading to demyelination.

4. Methods

4.1. Ethics statement

Use of animals and all experimental procedures were reviewed and approved by *the Institutional Animal Care and Use Committee* at the University of Pennsylvania, Philadelphia. Animal protocols adhered to the guidelines of the United States National Institutes of Health Office of Laboratory Animal Welfare Guide for the Care and Use of Laboratory Animals, 8th Edition. All experimental methods were carried out in "accordance" with the approved guidelines of Universities of Pennsylvania, USA.

4.2. Viruses

Recombinant isogenic DM strain of MHV, RSA59, and NDM strain RSMHV2 were described previously [5,48]. RSA59 and RSMHV2 are isogenic except for the spike gene, which encodes an envelope glycoprotein [49–51]. Each strain also expresses enhanced green fluorescence protein (EGFP) [48].

4.3. Inoculation

Four-week-old, MHV-free, C57BL/6 mice (Jackson Laboratory) were inoculated intracranially with 50% LD_{50} dose of RSA59 (20,000 PFU) or RSMHV2 (100 PFU) as described previously [5,48]. Mock-infected controls were inoculated with an uninfected cell lysate at a comparable dilution. Animals were sacrificed (five mice per group) at day 6 or 7 (acute stage) and day 25 or 26 (chronic stage) post-infection (p.i.).

We have shown in a series of prior studies that these vastly differing inoculation doses are used because they indeed result in in similar levels of viral replication, infection, liver pathology and viral spread.

Briefly, our previous studies demonstrated that different doses of the viral strains (RSA59, 20,000 PFU versus RSMHV2, 100 PFU) do not affect neural cell infection and inflammation within the brain [5]. The two very distinct and different doses of viruses used are based on 50% of the LD50, where previously it has been demonstrated that both strains replicate at a similar rate in the brain and spinal cord and viral titers at day 5 and day 7 p.i. are almost the same [4,6,52]. Moreover, even at 100 PFUs inoculation, RSA59 can cause demyelination although the number and size of demyelinating plaques formed was less compared to an inoculum of 20,000 PFUs [4].

4.4. RNA isolation and Affymetrix microarray

For microarray analysis, total RNA was isolated from spinal cords of RSA59, RSMHV2 and mock-infected mice using the Qiagen RNeasy mini kit and DNase treatment. cDNA was synthesized using the Ovation Pico WTA system V2 (Nugen Technologies), fragmented, and labeled with biotin followed by hybridization with Affymetrix gene chip mouse gene 1.0 ST array that contains 750,000 unique 25mer oligonucleotide features for 28,000 gene level probe sets. Arrays were washed and stained using GeneChip fluidics station 450 and hybridization signals were amplified using antibody amplification with goat IgG (Sigma-Aldrich) and anti-streptavidin biotinylated antibody (Vector Laboratories). Chips were scanned in GeneChip scanner 3000 7G. Cel files corresponding to scanned spots were created using Command Console software, and loaded into Genespring Software (Agilent) to identify differentially expressed genes and for statistical analysis. Background correction and normalization was performed using Robust Multichip

Average in Genespring software. Volcano plots were used to identify differentially expressed genes using unpaired 2-sample student t-tests taking p-values ≤0.05 and a fold change of ≥1.5 or ≥2 as indicated. Gene lists were then loaded into the Ingenuity Pathway Analysis software (IPA) for network and functional analysis.

4.5. Real time quantitative PCR

Total RNA was isolated from spinal cord tissue of DM, NDM and mock-infected mice on day 6 and day 25 p.i. using a Qiagen RNeasy mini kit after transcardial perfusion. cDNA was synthesized using High capacity cDNA reverse transcription kit (Applied Biosystems). Real time PCR was performed using Taqman real time PCR master mix (Applied Biosystems) and Taqman Primer probe set (Supplementary Table 4) in an ABI PRISM 7000 Sequence Detection System. Average Ct values were calculated from triplicate reactions and were normalized with β-actin Ct values. The relative fold change in DM and NDM infected mice with respect to mock-infected was obtained by calculating the $2^{-\Delta\Delta Ct}$ values and plotted. One way ANOVA was used to determine the upregulation of genes in DM, NDM infected mice with respect to mock infected mice and between the strains. Levels of significance were determined on the basis of multiple comparison testing.

4.6. Protein extraction

150 mg of flash frozen tissue was lysed in 1 mL of lysis buffer (RIPA buffer containing 0.1% SDS and 0.1% Triton X-100 with complete mini protease inhibitor cocktail tablets (#11836153001; Roche). Spinal cord tissues were homogenized by trituration followed by sonication and centrifuged at 13,500 RPM for 10 min at 4 °C. Protein concentration was measured by BCA kit in a microplate reader (Wallac Victor 2 1420 Multicounter; Perkin Elmer).

4.7. Multiplex array system

Mouse cytokine assay was performed for Th1 and Th2 cytokines using MesoScale Discovery (MSD) 96 well Multi-Spot Mouse TH1/TH2 9-Plex Ultrasensitive Kit and IL-6 Ultrasensitive Kit (MSD Biomarker assay system). Brain and spinal cord homogenates were tested at 250 μg and 50 μg per well. After 2 h incubation, plates were washed three times with PBS + 0.05% Tween-20. 25 μL of 1× Detection Antibody Solution was added into each well and incubated for 2 h with shaking at room temperature. Plates were washed 3 times with PBS + 0.05% Tween-20. 150 μL of 2× Read Buffer was added to each well. Data was acquired in SECTOR® Imager and analyzed using MSD Workbench software. Two way ANOVA was used to determine the changes in protein expression in DM and NDM strain infected mice with respect to mock infected mice as well as between the strains. Levels of significance were determined on the basis of multiple comparison testing.

4.8. Histopathology and immunohistochemistry

Mice were sacrificed at day 6 and day 25 p.i. and perfused transcardially with PBS followed by 4% paraformaldehyde. Liver, brain and spinal cord were harvested, embedded in paraffin, sectioned, and stained with hematoxylin and eosin [53]. For evaluating demyelination, spinal cord sections were stained with luxol fast blue. To examine inflammation (microglia/macrophage upregulation), immunohistochemistry of brain and spinal cord sections was performed with Iba1 antibody using the avidin biotin immunoperoxidase technique (ABC kit, Vector laboratories,) and 3,3′ diaminobenzidine substrate [54]. Half of liver and spinal cord tissues from each mouse used for RNA extraction were also processed for histopathological analysis.

4.9. Pathway and statistical analyses

Data analyses were performed using GeneSpring software version 12.0 (Agilent Technologies, Inc., Santa Clara, CA). Probe set signals were calculated with the Iterative Plier 16 summarization algorithm; with the baseline to median of all samples used as the baseline option. Data was filtered by percentile and a lower cut off was set at 25. The criteria for identifying a gene as being differentially expressed were set at ≥2-fold (for day 25 p.i. data set) and >1.5-fold (for day 6 p.i. data set) changes as indicated. Statistical analysis was performed to compare 2 groups using unpaired t-tests, with significance inferred by p-values less than or equal to 0.05.

Volcano plots were used to identify differentially expressed genes using unpaired 2-sample student t-tests taking p-values ≤0.05 and a fold change of ≥1.5 or ≥2 as indicated. The list of differentially expressed genes was loaded into Ingenuity Pathway Analysis (IPA) 8.0 software (http://www.ingenuity.com) to perform biological network and functional analyses per software instructions.

Supplementary data to this article can be found online at http://dx.doi.org/10.1016/j.clim.2016.07.004.

Author contribution

KB and DC participated in data analysis and data interpretation and drafted the manuscript.

RK and JDS performed all animal experiments. SA performed all the affymetirx microarray experiments and provided help to KB and DC for data analysis and data interpretation.

Mouse cytokine assay was performed by AC and JDS. LK blindly read the pathological samples. KSS and RJC made substantial contributions to experimental design, and were involved in data analysis and critical revisions of the manuscript. JDS led all aspects of this work including experimental design, participated in or supervised all experimental procedures, analyzed and interpreted data and critically revised the manuscript.

Competing financial interest

The authors declare no competing financial interests.

Acknowledgements

This work is supported by Research Grant [BT/PR14260/MED/30/437/2010, BT/PR4530/MED/30/715/2012] from Department of Biotechnology India, Indian Institute of Science Education and Research-Kolkata (IISER-K), India start up Fund to JDS; and NIH grant [EY015014] and Research to Prevent Blindness funding to KSS. This work is also partially supported by 2013 ASM-IUSSTF Indo-US Research Professorship Award to JDS and RC to develop bi-lateral research relationship between India and US. We thank University Grants Commission (UGC) for providing the research support to KB and DC. Authors thank the Cancer Genomics Center, Thomas Jefferson University, Philadelphia, USA for Gene Chip Microarray facility. Authors also thank Mr. Manmeet Singh and Mr. Subhajit Das Sarma for statistical analysis in the blinded fashion.

References

[1] J.H. Noseworthy, C. Lucchinetti, M. Rodriguez, B.G. Weinshenker, Multiple sclerosis, N. Engl. J. Med. 343 (2000) 938–952.
[2] E. Lavi, D.H. Gilden, M.K. Highkin, S.R. Weiss, Persistence of mouse hepatitis virus A59 RNA in a slow virus demyelinating infection in mice as detected by in situ hybridization, J. Virol. 51 (1984) 563–566.
[3] S.J. Das, A mechanism of virus-induced demyelination, Interdiscip. Perspect. Infect. Dis. 2010 (2010) 109239.
[4] J. Das Sarma, L. Fu, J.C. Tsai, S.R. Weiss, E. Lavi, Demyelination determinants map to the spike glycoprotein gene of coronavirus mouse hepatitis virus, J. Virol. 74 (2000) 9206–9213.

[5] J. Das Sarma, K. Iacono, L. Gard, R. Marek, L.C. Kenyon, M. Koval, et al., Demyelinating and nondemyelinating strains of mouse hepatitis virus differ in their neural cell tropism, J. Virol. 82 (2008) 5519–5526.
[6] J. Das Sarma, L.C. Kenyon, S.T. Hingley, K.S. Shindler, Mechanisms of primary axonal damage in a viral model of multiple sclerosis, J. Neurosci. 29 (2009) 10272–10280.
[7] K.S. Shindler, L.C. Kenyon, M. Dutt, S.T. Hingley, S.J. Das, Experimental optic neuritis induced by a demyelinating strain of mouse hepatitis virus, J. Virol. 82 (2008) 8882–8886.
[8] K.S. Shindler, D. Chatterjee, K. Biswas, A. Goyal, M. Dutt, M. Nassrallah, et al., Macrophage-mediated optic neuritis induced by retrograde axonal transport of spike gene recombinant mouse hepatitis virus, J. Neuropathol. Exp. Neurol. 70 (2011) 470–480.
[9] D. Chatterjee, S. Addya, R.S. Khan, L.C. Kenyon, A. Choe, R.J. Cohrs, et al., Mouse hepatitis virus infection upregulates genes involved in innate immune responses, PLoS One 9 (2014), e111351.
[10] R. Elliott, F. Li, I. Dragomir, M.M. Chua, B.D. Gregory, S.R. Weiss, Analysis of the host transcriptome from demyelinating spinal cord of murine coronavirus-infected mice, PLoS One 8 (2013), e75346.
[11] S. Navas, S.H. Seo, M.M. Chua, J. Das Sarma, E. Lavi, S.T. Hingley, et al., Murine coronavirus spike protein determines the ability of the virus to replicate in the liver and cause hepatitis, J. Virol. 75 (2001) 2452–2457.
[12] D. Ito, K. Tanaka, S. Suzuki, T. Dembo, Y. Fukuuchi, Enhanced expression of Iba1, ionized calcium-binding adapter molecule 1, after transient focal cerebral ischemia in rat brain, Stroke 32 (2001) 1208–1215.
[13] G.W. Simmons, W.W. Pong, R.J. Emnett, C.R. White, S.M. Gianino, F.J. Rodriguez, et al., Neurofibromatosis-1 heterozygosity increases microglia in a spatially and temporally restricted pattern relevant to mouse optic glioma formation and growth, J. Neuropathol. Exp. Neurol. 70 (2011) 51–62.
[14] E. Lavi, D.H. Gilden, M.K. Highkin, S.R. Weiss, Detection of MHV-A59 RNA by in situ hybridization, Adv. Exp. Med. Biol. 173 (1984) 247–257.
[15] S. Perlman, G. Jacobsen, A.L. Olson, A. Afifi, Identification of the spinal cord as a major site of persistence during chronic infection with a murine coronavirus, Virology 175 (1990) 418–426.
[16] G.P. Owens, J.L. Bennett, D.H. Gilden, M.P. Burgoon, The B cell response in multiple sclerosis, Neurol. Res. 28 (2006) 236–244.
[17] G.P. Owens, D. Gilden, B. MP, X. Yu, B. JL, Viruses and Multiple Sclerosis, Neuroscientist (2011).
[18] D.H. Gilden, Infectious causes of multiple sclerosis, Lancet Neurol. 4 (2005) 195–202.
[19] J.J. Archelos, M.K. Storch, H.P. Hartung, The role of B cells and autoantibodies in multiple sclerosis, Ann. Neurol. 47 (2000) 694–706.
[20] A.H. Cross, J.L. Trotter, J. Lyons, B cells and antibodies in CNS demyelinating disease, J. Neuroimmunol. 112 (2001) 1–14.
[21] D. Lambracht-Washington, K.C. O'Connor, E.M. Cameron, A. Jowdry, E.S. Ward, E. Frohman, et al., Antigen specificity of clonally expanded and receptor edited cerebrospinal fluid B cells from patients with relapsing remitting MS, J. Neuroimmunol. 186 (2007) 164–176.
[22] M.J. Walsh, J.M. Murray, Dual implication of 2′,3′-cyclic nucleotide 3′ phosphodiesterase as major autoantigen and C3 complement-binding protein in the pathogenesis of multiple sclerosis, J. Clin. Invest. 101 (1998) 1923–1931.
[23] A. Corcione, S. Casazza, E. Ferretti, D. Giunti, E. Zappia, A. Pistorio, et al., Recapitulation of B cell differentiation in the central nervous system of patients with multiple sclerosis, Proc. Natl. Acad. Sci. U. S. A. 101 (2004) 11064–11069.
[24] S. Ragheb, Y. Li, K. Simon, S. VanHaerents, D. Galimberti, M. De Riz, et al., Multiple sclerosis: BAFF and CXCL13 in cerebrospinal fluid, Mult. Scler. 17 (2011) 819–829.
[25] B. Serafini, B. Rosicarelli, R. Magliozzi, E. Stigliano, F. Aloisi, Detection of ectopic B-cell follicles with germinal centers in the meninges of patients with secondary progressive multiple sclerosis, Brain Pathol. 14 (2004) 164–174.
[26] J. Das Sarma, L.C. Kenyon, S.T. Hingley, K.S. Shindler, Mechanisms of primary axonal damage in a viral model of multiple sclerosis, J. Neurosci. 29 (2009) 10272–10280.
[27] D. Chatterjee, K. Biswas, S. Nag, S.G. Ramachandra, S.J. Das, Microglia play a major role in direct viral-induced demyelination, Clin. Dev. Immunol. 2013 (2013) 510396.
[28] C.C. Bergmann, T.E. Lane, S.A. Stohlman, Coronavirus infection of the central nervous system: host-virus stand-off, Nat. Rev. Microbiol. 4 (2006) 121–132.
[29] C.C. Bergmann, B. Parra, D.R. Hinton, R. Chandran, M. Morrison, S.A. Stohlman, Perforin-mediated effector function within the central nervous system requires IFN-gamma-mediated MHC up-regulation, J. Immunol. 170 (2003) 3204–3213.
[30] F.S. Cheever, J.B. Daniels, et al., A murine virus (JHM) causing disseminated encephalomyelitis with extensive destruction of myelin, J. Exp. Med. 90 (1949) 181–210.
[31] T.E. Lane, M.P. Hosking, The pathogenesis of murine coronavirus infection of the central nervous system, Crit. Rev. Immunol. 30 (2010) 119–130.
[32] C. Ramakrishna, S.A. Stohlman, R.D. Atkinson, M.J. Shlomchik, C.C. Bergmann, Mechanisms of central nervous system viral persistence: the critical role of antibody and B cells, J. Immunol. 168 (2002) 1204–1211.
[33] J.D. Rempel, S.J. Murray, J. Meisner, M.J. Buchmeier, Differential regulation of innate and adaptive immune responses in viral encephalitis, Virology 318 (2004) 381–392.
[34] A.L. Croxford, F.C. Kurschus, A. Waisman, Mouse models for multiple sclerosis: historical facts and future implications, Biochim. Biophys. Acta 2011 (1812) 177–183.
[35] B. Kornek, M.K. Storch, R. Weissert, E. Wallstroem, A. Stefferl, T. Olsson, et al., Multiple sclerosis and chronic autoimmune encephalomyelitis: a comparative quantitative study of axonal injury in active, inactive, and remyelinated lesions, Am. J. Pathol. 157 (2000) 267–276.
[36] L. Steinman, S.S. Zamvil, How to successfully apply animal studies in experimental allergic encephalomyelitis to research on multiple sclerosis, Ann. Neurol. 60 (2006) 12–21.
[37] R.T. Johnson, The virology of demyelinating diseases, Ann. Neurol. 36 (Suppl) (1994) S54–S60.
[38] W.A. Sibley, C.R. Bamford, K. Clark, Clinical viral infections and multiple sclerosis, Lancet 1 (1985) 1313–1315.
[39] S.J. Das, Microglia-mediated neuroinflammation is an amplifier of virus-induced neuropathology, J. Neurovirol. 20 (2014) 122–136.
[40] A. Kishore, A. Kanaujia, S. Nag, A.M. Rostami, L.C. Kenyon, K.S. Shindler, et al., Different mechanisms of inflammation induced in virus and autoimmune-mediated models of multiple sclerosis in C57BL6 mice, BioMed. Res. Int. 2013 (2013) 589048.
[41] E. Lavi, D.H. Gilden, Z. Wroblewska, L.B. Rorke, S.R. Weiss, Experimental demyelination produced by the A59 strain of mouse hepatitis virus, Neurology 34 (1984) 597–603.
[42] C. Lucchinetti, W. Bruck, J. Parisi, B. Scheithauer, M. Rodriguez, H. Lassmann, Heterogeneity of multiple sclerosis lesions: implications for the pathogenesis of demyelination, Ann. Neurol. 47 (2000) 707–717.
[43] A.A. Dandekar, G.F. Wu, L. Pewe, S. Perlman, Axonal damage is T cell mediated and occurs concomitantly with demyelination in mice infected with a neurotropic coronavirus, J. Virol. 75 (2001) 6115–6120.
[44] S.D. Miller, C.L. Vanderlugt, W.S. Begolka, W. Pao, R.L. Yauch, K.L. Neville, et al., Persistent infection with Theiler's virus leads to CNS autoimmunity via epitope spreading, Nat. Med. 3 (1997) 1133–1136.
[45] H.L. Lipton, Theiler's virus infection in mice: an unusual biphasic disease process leading to demyelination, Infect. Immun. 11 (1975) 1147–1155.
[46] M.C. Dal Canto, R.W. Melvold, B.S. Kim, S.D. Miller, Two models of multiple sclerosis: experimental allergic encephalomyelitis (EAE) and Theiler's murine encephalomyelitis virus (TMEV) infection. A pathological and immunological comparison, Microsc. Res. Tech. 32 (1995) 215–229.
[47] L.P. Weiner, R.T. Johnson, R.M. Herndon, Viral infections and demyelinating diseases, N. Engl. J. Med. 288 (1973) 1103–1110.
[48] J. Das Sarma, E. Scheen, S.-H. Seo, M. Koval, S.R. Weiss, Enhanced green fluorescent protein expression may be used to monitor murine coronavirus spread in vitro and in the mouse central nervous system, J. Neurovirol. 8 (2002) 381–391.
[49] T.M. Gallagher, M.J. Buchmeier, Coronavirus spike proteins in viral entry and pathogenesis, Virology 279 (2001) 371–374.
[50] Z. Qiu, S.T. Hingley, G. Simmons, C. Yu, J. Das Sarma, P. Bates, et al., Endosomal proteolysis by cathepsins is necessary for murine coronavirus mouse hepatitis virus type 2 spike-mediated entry, J. Virol. 80 (2006) 5768–5776.
[51] E. Lavi, Q. Wang, S.R. Weiss, N.K. Gonatas, Syncytia formation induced by coronavirus infection is associated with fragmentation and rearrangement of the Golgi apparatus, Virology 221 (1996) 325–334.
[52] L.C. Kenyon, K. Biswas, K.S. Shindler, M. Nabar, M. Stout, S.T. Hingley, et al., Gliopathy of demyelinating and non-demyelinating strains of mouse hepatitis virus, Front. Cell. Neurosci. 9 (2015) 488.
[53] J.D.S.S. Das Sarma, K. Chatterjee, T. Dalui, S. Ghosh, Tissue specific optimization of Haematoxylin and eosin stain: an experiment accomplished by varying the period of fixation and duration of stain. Online journal of biosciences and informatics, Online J. Biosci. Inform. 4 (2013) 64–81.
[54] S.C.K. Das Sarma, H. Dinda, D. Chatterjee, S.J. Das, Cytomorphological and cytochemical identification of microglia, ISRN Immunology, 2013;Volume 2013, 2013.